Konya Mühendislik Bilimleri Dergisi., c. 13, s. 4, 1279-1289, 2025
Konya Journal of Engineering Sciences v. 13, n. 4, 1279-1289, 2025
ISSN: 2667-8055 (Electronic)
DOI: 10.36306/konjes.1737771

PROCESS CONTROL AGENT EFFECT ON Mg PARTICLES DURING HIGH ENERGY BALL MILLING

[1,*] Halit SÜBÜTAY, [2] İlyas ŞAVKLIYILDIZ

[1] *Selçuk University, Metallurgical and Materials Engineering Department, Konya, TÜRKİYE*
[2] *Konya Technical University, Metallurgical and Materials Engineering Department, Konya, TÜRKİYE*
[1] halit.subutay@selcuk.edu.tr, [2] isavkliyildiz@ktun.edu.tr

Highlights

- Mg powder was milled via high-energy ball milling with PCAs for various durations.
- SEM and XRD characterizations of the powders were performed.
- Methanol breaks flake morphology after 4h while stearic acid maintains up to 10h.
- Stearic acid favors proper mechanical alloying even at longer milling durations.
- No contamination or oxidation is detected in both systems.

Graphical Abstract

Overview of Experimental Methodology

***Corresponding Author:** Halit SÜBÜTAY, halit.subutay@selcuk.edu.tr

Konya Mühendislik Bilimleri Dergisi., c. 13, s. 4, 1279-1289, 2025
Konya Journal of Engineering Sciences v. 13, n. 4, 1279-1289, 2025
ISSN: 2667-8055 (Electronic)
DOI: 10.36306/konjes.1737771

PROCESS CONTROL AGENT EFFECT ON Mg PARTICLES DURING HIGH ENERGY BALL MILLING

[1,*] Halit SÜBÜTAY, [2] İlyas ŞAVKLIYILDIZ

[1] Selçuk University, Metallurgical and Materials Engineering Department, Konya, TÜRKİYE
[2] Konya Technical University, Metallurgical and Materials Engineering Department, Konya, TÜRKİYE
[1] halit.subutay@selcuk.edu.tr, [2] isavkliyildiz@ktun.edu.tr

(Received: 08.07.2025; Accepted in Revised Form: 01.09.2025)

ABSTRACT: This study surveys the outcome of different process control agents (PCAs) on the morphology of pure magnesium (Mg) powders along high-energy ball milling, focusing on milling duration. Milling up to 4 hours promotes platelet-like structures in Mg particles due to frequent collisions among balls, powder, and chamber walls, increasing particle size from 30 μm to 300 μm. Prolonged milling then causes fragmentation and reduces particle size. Comparative analysis of stearic acid and methanol reveals contrasting behaviors. Stearic acid preserves the flake morphology of Mg up to 10 hours, while methanol, due to its volatility, evaporates earlier in the process. This early loss of methanol leads to morphological breakdown before the mechanical alloying process completes. Thus, stearic acid provides better stability for extended milling durations. X-ray diffraction (XRD) analysis indicates texture formation along the (002) plane in both PCA systems, influenced by cold welding, work hardening, and rolling mechanisms. No oxidation or contamination is observed in either case after 12 hours of milling, confirming effective control of the milling environment. These results underline the importance of selecting an appropriate PCA based on its volatility and interaction with the Mg system to ensure efficient and contamination-free mechanical alloying.

Keywords: *Ball Milling, Magnesium, Powder Morphology, PCA*

1. INTRODUCTION

Being the lightest structural materials, magnesium (Mg) and its alloys have been extensively employed in fields such as aerospace, telecommunication, medical implants, and automotive engineering, owing to their well castability, superior energy absorption capability, and high specific strength [1-3]. The primary drawback of magnesium is its poor formability at ambient temperatures, primarily due to the restricted activation of slip systems[4]. In efforts to enhance the formability of magnesium and its alloys, researchers have explored various approaches. Among these, particularly rare earth elements (REs) such as: Ce[5], Y[6], Gd[7], Dy[8] the incorporation of alloying elements within the material's chemistry has been proposed as a viable strategy [9, 10] in addition to conventional thermomechanical treatments. These alloying methods, along with techniques like high-energy ball milling, have significantly contributed to improving property such as specific strength, creep resistance, and heat resistance [9].

High-energy ball milling (mechanical alloying) is a preferred method to increase the mechanical properties, especially where Mg must be used unalloyed and pure[11]. Mechanical alloying is one of the most famous overbalance operations for generation more homogeneous refined microstructures and enlarged solid solutions [12]. Furthermore, milling process also help us to adjust particle morphology and particle size distribution [13]. This method mentioned is a complicated process including the optimization of many variables to obtain a homogeneous microstructure or phase[14]. Atomic-scale milling and alloying can be obtained via perpetual cold welding, fracture and deformation [15-17]. The main parameters affecting the powder morphology in ball milling; size of starting powder, mechanical alloying speed and time, ball powder ratio, ball size, process control agent (PCA) and its amount etc.[18].

***Corresponding Author:** Halit SÜBÜTAY, halit.subutay@selcuk.edu.tr

The incorporation of a PCA during ball milling has been shown to effectively suppress severe cold welding by reducing surface energy, thereby facilitating a more pronounced reduction in particle size [19, 20]. Furthermore, the presence of PCA hinders excessive friction between the milling balls and the jar walls, which in turn minimizes wear and consequently reduces contamination [21]. The milled particles could have platelet structure due to cold welding. However, continuous fracturing-cold welding phenomenon on particles is supposed to be exist to reach proper milling conditions [22]. Thus, PCA becomes very crucial to mitigate cold welding effect on powder particles.

Methanol[23], n-hexane[24], stearic acid[25], oleic acid[26], ethanol[27], toluene[28], etc., are surfactants or process control agents added to stabilize the reactions. PCAs mainly have organic nature working as a surface active agents on particle surface [29]. The PCA located on particle surface has the role of alternating surface tension which eventually determines cold welding behavior of powder particles during ball milling process [30].

Depending on the materials system and milling duration, a high temperature rise could be expected during milling process. So, melting and evaporation points for PCA is crucial to determine milling conditions [31]. Because some PCAs could be volatized before ball milling process completed. Removal PCA from system could result cold welding and or storage of excessive compression stress on particles which lower the sinterability behavior ball milled powder [32]. Furthermore, PCAs are mainly organic compounds which contain carbon, oxygen and hydrogen [30]. Local excessive temperature rise during ball milling process could trigger decomposition of PCA and/or reaction of carbon and oxygen with milled metallic powders [33]. Thus, it is possible to observe the formation of carbides or oxides on the surface of particles which eventually affect the properties of final products [34, 35]. Overall, it is important to right PCA for ball milling process depending on the materials system and volatilization behavior of its PCA [36]. On the other hand, the amount of PCA injected system is also manage the morphology of the milled powder particles [37]. Adding varies PCA concentration differentiate the size of particles and evolve the particle shape from platelet structure to spherical morphology [38].

There are not many publications in the literature regarding the effect of different PCA systems on the particle size and shape of the powder on the high energy ball milling system of pure mg powder.

Generally, different ball milling parameters were investigated using a binary alloy system or a single PCA rather than pure material. In this study, the effect of two different PCA systems on the particle size and shape of pure Mg powder during high-energy ball milling and the lubricating and crushing effects of PCAs used were investigated.

2. MATERIAL AND METHODS

In this study, methanol (purity of 99.6%; Sigma-Aldrich, Germany) and stearic acid (purity of 98%, Tekkim, Türkiye) were employed to investigate the effect of PCA on the powder morphology of Mg particles during ball milling process. Pure Mg (99.95 wt% purity) powder was purchased by Nanografi Company, Türkiye. The average particle size of the as-received Mg powders was measured to be approximately 50 μm using a Malvern Instruments Mastersizer 2000e particle size analyzer. The Mg powders were milled in mechanical alloying device (Retsch PM 200) under and inert Ar gas atmosphere in different milling time (0,5 h, 1 h, 2 h, 3 h, 5 h, 8 h, 10 h and 12 h) at milling speed of 300 rpm. Ball-to-powder (BPR) ratio was selected as 10:1, and 10 mm diameter WC balls in a WC jar (125 ml) were employed in the ball milling operation. Methanol and stearic acid were employed as PCAs at a concentration of 2 wt. %. Figure 1a and 1b schematically illustrate the milling process and the scanning electron microscopy (SEM) image of the as-received Mg powder, respectively.

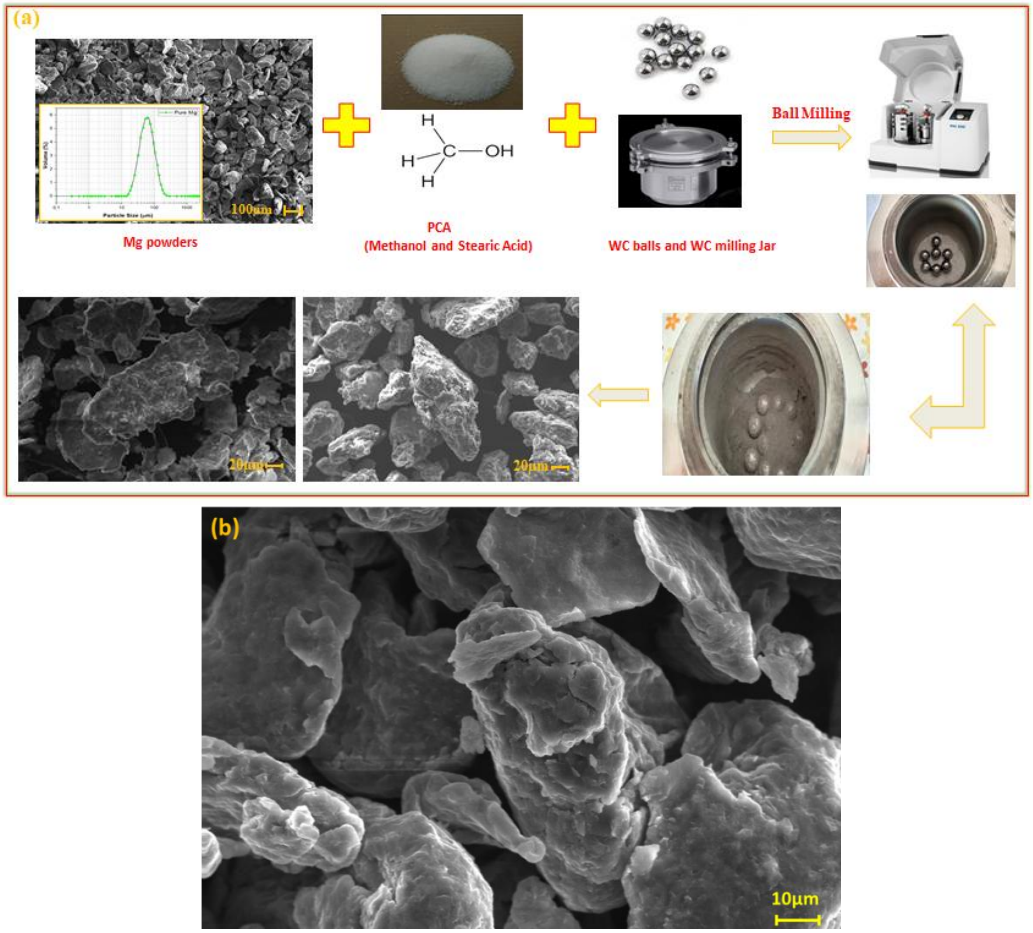

Figure 1 a) Overview of the Experimental Methodology, b) pure Mg SEM image

The morphological development of the milled powders was characterized using a SEM (ZEISS EVO 10). In addition, the elemental distribution and possible presence of impurities were evaluated through energy-dispersive X-ray spectroscopy (EDS) mapping. To identify crystalline phases and assess crystallographic texture and changes in behavior of the crystallinity in particle, X-ray diffraction (XRD) analysis was performed using a Rigaku ZSX Primus-II system. Diffraction data were acquired employing Cu-Kα radiation (λ = 0.15406 nm), with measurements conducted via a step-scan mode at 0.15° intervals in 2θ and a dwelling time of 1 second per step

3. RESULTS AND DISCUSSION

3.1. Effect of Methanol on Mg powder morphology with different milling duration

In the present section, the effect of PCA is investigated as a function of different milling duration. Figure 2 includes SEM micrographs of Mg powders processed by methanol with different durations up to 12 h. The figure 2a shows that Mg powder mixed with methanol first preserves its powder morphology after 30 min ball milling process which suggests that 30 ball milling process has no effect on powder morphology in this case. However, Mg powders start to become flat after 1h milling duration as seen in Figure 2a. The collision of powders between ball to ball and ball to wall leads to such morphological change on powder. Because continuous collision events ball milling process triggers plastic deformation mechanisms on Mg powders. Cold working, work hardening and rolling are the few mechanisms thrives flat particle structure shown on SEM micrographs. Further ball milling process up to 2h improves the flat morphology of powder and bigger flat powders arouse as illustrated in Figure 2c. Besides, there are integrated particles one to another in some regions which are stated as cold welding

between particles due to ball milling. The particle integration is induced and improved with increasing ball milling time a seen in Figure 2d. Most particles look like cold welded to each other and create new platelets or flake shape particles. Such particles are generated with specific directions such as (002) for Mg and its alloys and (110) direction for Al and its alloys [39] depending on the crystal structure of materials system. For Mg alloys, (002) direction is known as c direction in which weak bonds exist. So, many literature data reveal this familiar behavior which is observed in XRD analysis for our study which will be mentioned further sections of this paper. Furthermore, such integration due to continuous collision during ball milling process could also lead to a twining mechanism as a new grain boundary mechanism.

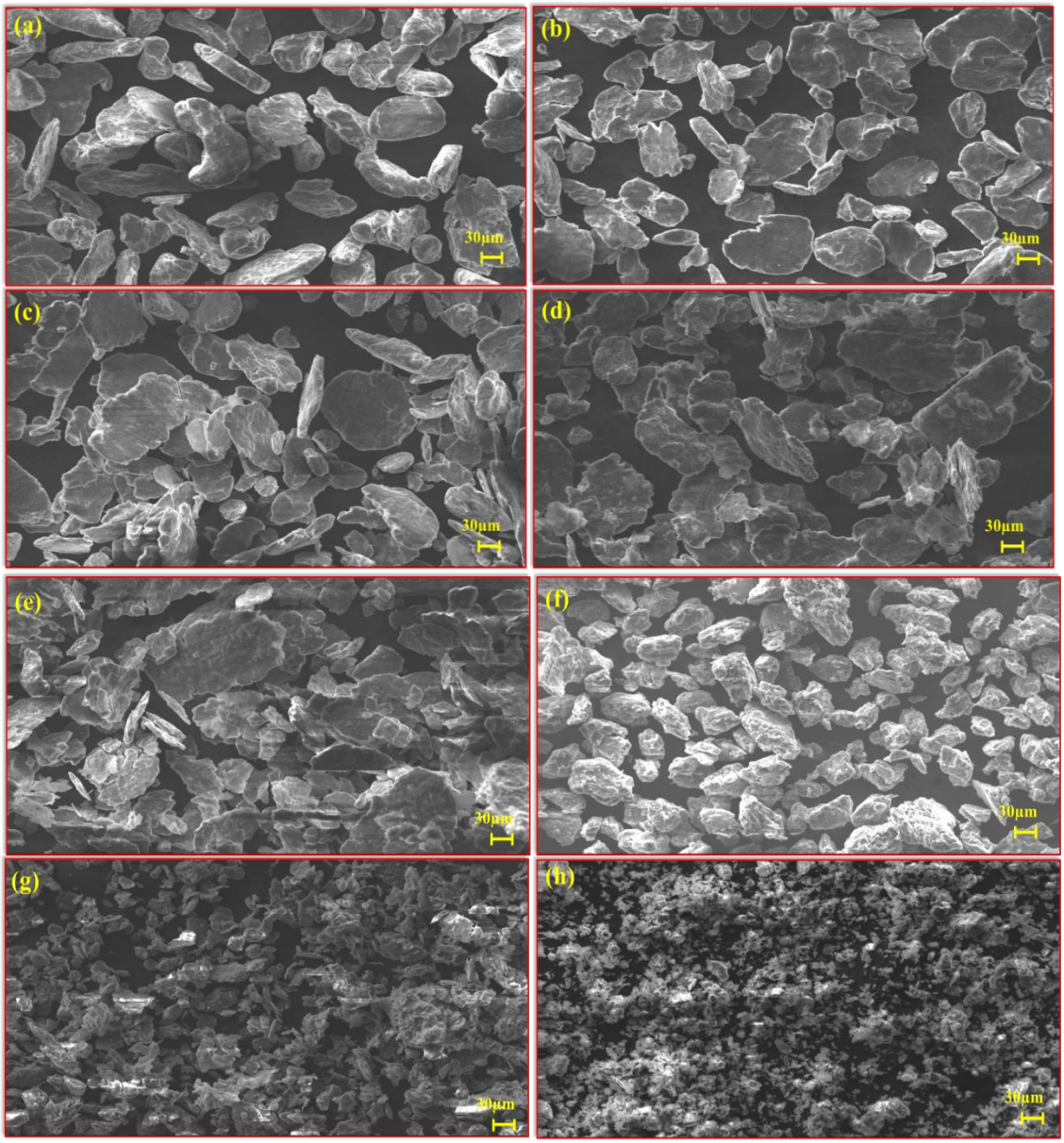

Figure 2 SEM investigation of ball milled powders with methanol at different milling durations a) 30 min., b) 1h, c) 2h, d) 3h, e) 5h, f) 8h, g) 10h and h) 12h. [40]

The platelet structure for Mg particles is enhanced for increasing ball milling up **to 4h (Figure 2e)** and the flake particles are approximately reaches up to 250 microns which is huge number comparing with initial particle size of Mg powder (50 microns). However, further milling process after 4h reveals a singularity on particle morphology of Mg. When the milling duration reaches the 8h, the platelet or flake

structure of particles breaks into smaller and rounded form as illustrated in Figure 2f. The monomodal particle size distribution is also observed instead of bimodal distribution which is not desired or useful for sintering the green dense Mg powders into highly dense bulk form. A closer look to Figure 2g and h suggests that the particle morphology break into much smaller form. Milling process of 10h diminishes the particle size of Mg powder down to 30 microns. However, as illustrated in Figure 2g, there is still presence of flake particles which advice that both fracture and cold welding mechanism are still operational concomitantly. When the ball milling duration reaches 12h (Figure 2h), the powder morphology turns into small rounded particles and no platelet or flake particles are left. The particle size distribution is measured approximately 10 microns which is very low comparing the initial particle size of unprocessed Mg powder (50 microns). Overall, it can be stated that ball milling process with methanol process agent is viable to achieve smaller and monomodal particle size distribution.

3.2. Effect of Stearic acid on Mg powder morphology with different milling duration

In this section, the role of the stearic acid as a process control agent during ball milling process is evaluated. Figure 3 illustrates the particle morphology of Mg milled with stearic acid as a function of time up to 12h. At the beginning, short milling time (30 min) with stearic acid get involved action on powder by creating flake particles. Further ball milling up to 1h makes improvement on the flake structure and bigger flake particles is observed in Figure 3b. However, the 2h ball milling process shows singularity on particle morphology. The flake structure of the particles starts to integrate to each other due to excessive plastic deformation as seen Figure 3c. The integrated particles triggers twinning mechanism and create new grain boundary formation. Platelet particle morphology up to 300 microns is observed, which is relatively higher compared to the initial particle size of Mg (50 microns). Furthermore, the platelet morphology started break apart with 3h milling duration as shown Figure 3d. This phenomenon is the sign that the stearic acid as process control agent works properly in this issue. Two important mechanisms, cold welding and particle fracture, continuously arouse in this milling duration which also suggests proper ball milling process. Stearic acid plays crucial role to reduce the cold welding effect and leads to fracture mechanism on particles. Synergetic harmony of cold welding and fracture mechanism on particles is incessantly preserved with prolonging milling duration up to 8h (Figure 3e, f). On the other hand, distinguished particle morphology is observed with 10 h ball milling. The particles are broken down to 30 microns with flake structure which is smaller compared with the initial particles of Mg (50 microns). The cold welding and fracture mechanism is no longer operational with increasing ball milling up to 12h. Smaller particle form with monomodal distribution is eventually acquired with 12 h milling time which leads us ball milling process is completed.

3.3. Comparison of the effect of methanol and stearic acid on Mg powder morphology

In this section, the different behaviors of methanol and stearic acid are defined concomitantly. Figure 2 and 3 shows the contrast on the particle morphology with each process control agent. At the beginning, both methanol and stearic acid are functional on flake structure. A closer look to Figure 2 and 3 b reveals the different particle morphology depending on the PCA. 8h milling duration for methanol has a fracture effect on particles and the platelet structure turns into rounded smaller particles. On the other side, stearic acid with 8h milling duration still conducts the cold welding mechanism due to plastic deformation and bigger platelet structure is observed. The Figure 2 and 3 shows 12h milled powders with both methanol and stearic acid. Particles milled with methanol break down to 10 microns with rounded shapes.

However, the powder processed with stearic acid just breaks down to 30 microns and the shape of the particles preserves its flake structure. Many reasons have effects on the particle morphology due to PCA. Several PCA has organic structure so that this structure could be decompose at higher temperature and loses its function. Besides, each PCA has different melting and boiling points so that during high

energy ball milling, the system goes up to higher temperatures due to continuous collision. Eventually, the PCA could be evacuated due to lower volatilization temperature.

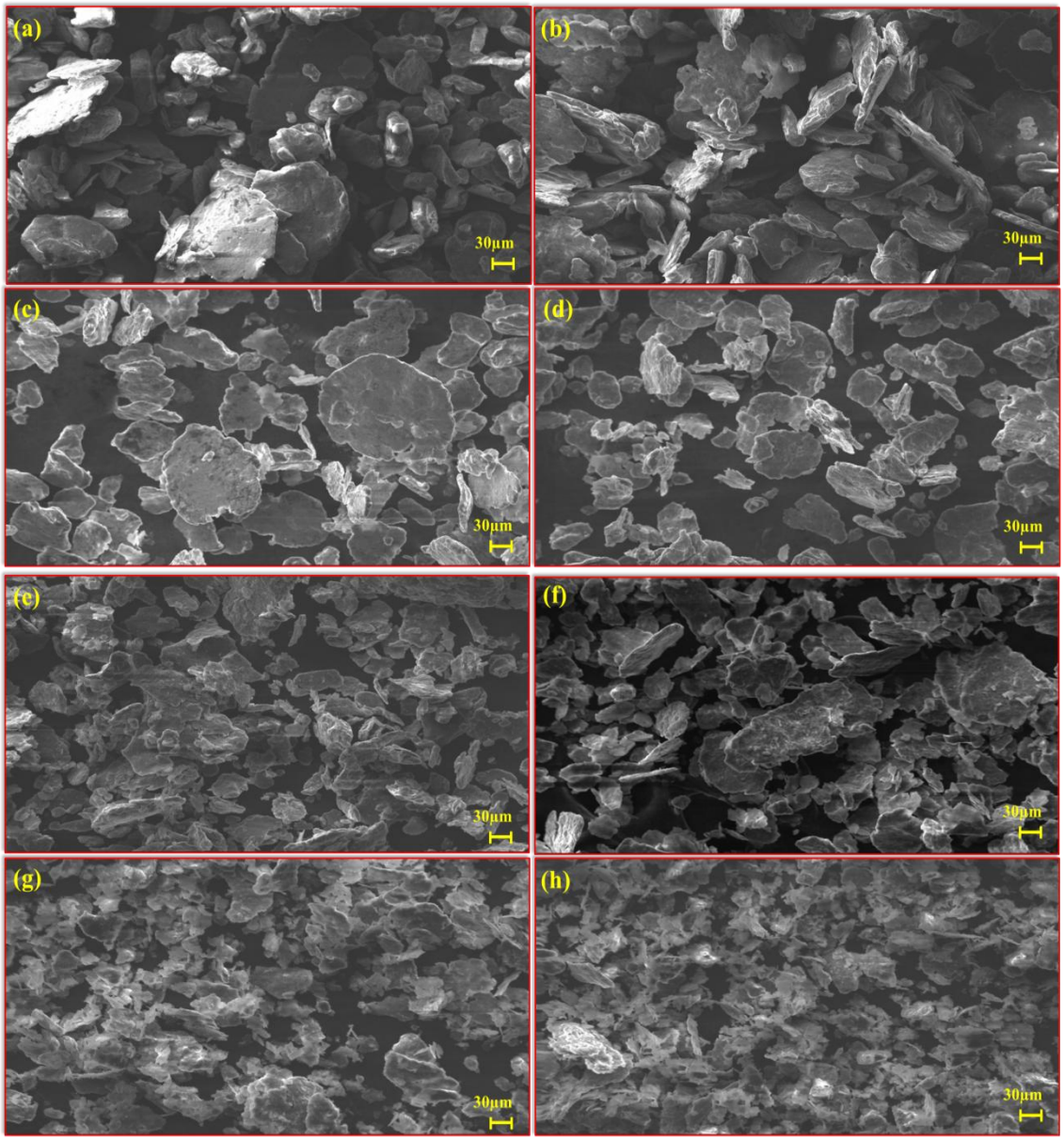

Figure 3 SEM investigation of ball milled powders with stearic acid at different milling durations a) 30 min., b) 1h, c) 2h, d) 3h, e) 5h, f) 8h, g) 10h and h) 12h [40].

3.4. XRD analysis of milled Mg powder morphology with different lubricants

Figure 4 represents XRD data spectra for milled samples with both stearic acid and methanol media. As a first glance, we only observe peak profiles which belong to metallic Magnesium. There is no extra peak formation observed due to contamination or any interaction between Mg and PCA. So, the high energy ball milling procedure for this study is carried out properly. However, the ball milled powders with different PCA shows singularity in terms of texture effect. As explained in previous sections, stearic acid has ability to make platelet structure on powder. So, the XRD data suggests that platelet structure is formed on (002) direction in hexagonal structure of Mg. The XRD spectrum of the powder milled by stearic acid reveals higher intensity (002) peak reflection than the main or major peak of (101) reflection.

However, ball milling with methanol lubricant agent leads to breaking the platelet structure. According to x-ray analysis, there is slight texture formation on (002) reflection comparing with un-milled powder but, due to nature of methanol, the texture formation on (002) direction is limited. The XRD data analysis helps us to verify crystallographic nature of platelet structure which is also observed on SEM micrograph examinations.

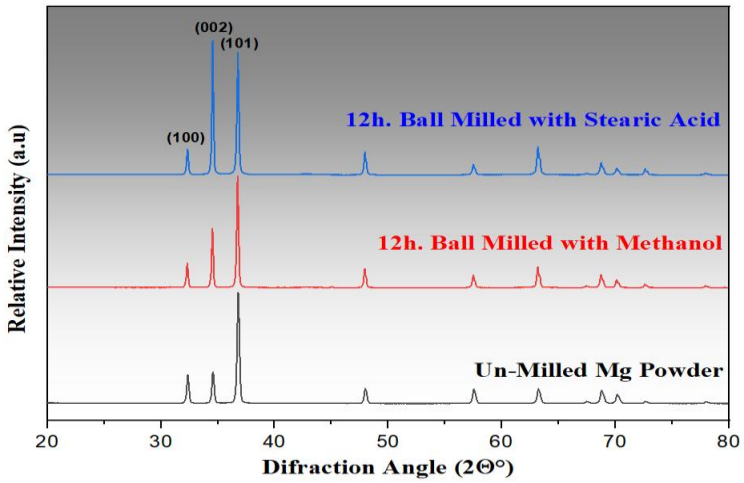

Figure 4 XRD spectra representation of Pure Mg and 12h ball milled Mg Powders with different PCA [40].

Figure 5 represents the EDS analysis of powders to investigate any impurities during ball milling process with existence of different lubricants. Because continuous collision between powder and balls creates high temperature rise and this high temperature formation triggers lubricant evaporation and chemical reaction between lubricant and the powder. Therefore this issue could cause contamination on milled powder. According Figure 5 a-b, we do not observe such contamination on milled powder manufacture by methanol and stearic acid. The high energy ball milling procedure for powders is carried out at atmosphere controlled setup. So, the EDS examinations showed in Figure 5 a-b exhibits mitigation for contamination from outer atmosphere as well.

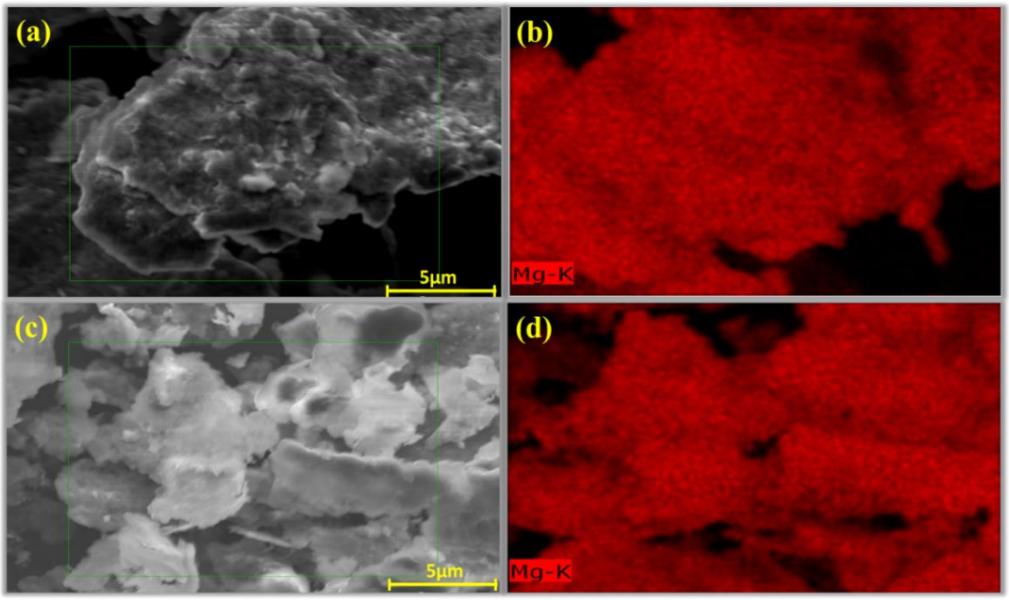

Figure 5 EDS analysis of ball milled powders for Methanol a) 8h.,; Stearic Acid c) 8h, conditions [40].

4. CONCLUSION

In this study, the effect of PCA is investigated with respect to high energy ball milling duration in Mg material systems. Following outcomes is acquired;

1- Methanol as PCA leads platelet powder morphology up 4h milling duration. Such a structure reveals texture formation on (002) crystallographic direction. In this stage the reality of ball milling issue triggers different mechanisms such as cold welding, work hardening and rolling etc. However, further milling process break these flake particles into smaller morphology.
2- Similar flake behavior for particles is also confirmed for the stearic acid condition. The stearic acid as PCA keeps such flake morphology up to 10h milling process. For 12h condition, we observe bimodal particle distribution with broken structures.
3- The methanol has more volatilization tendency comparing with stearic acid so that methanol could be evaporated at early stages of milling process so that the flake particles are broken into small pieces at shorter milling process.
4- Such differences between for methanol are not favorable because ball milling process ends before mechanical alloying completes.
5- After longer ball milling process for both systems, we do not observe any oxidation or contamination in the material system which reveals that the processes are completed optimum conditions.

Declaration of Ethical Standards

The authors declare that this study's materials and methods did not require approval from an ethics committee.

Credit Authorship Contribution Statement

The authors have contributed equally to this manuscript.

Declaration of Competing Interest

The authors declare that they have no conflicts of interest.

Funding / Acknowledgements

No funding information is available. This work originates from the Ph.D. thesis of Halit Sübütay, titled "Investigation of the Mechanical and In-Vivo Properties of Mg(1–X)SnX Alloys Produced by Mechanical Alloying."

Data Availability

The data supporting the findings of this study are available on request from the corresponding author.

REFERENCES

[1] Z. Aalipour *et al.*, "Strain dependency of dynamic recrystallization during thermomechanical processing of Mg-Gd-Y-Zn-Zr alloy," *journal of materials research and technology*, vol. 18, pp. 591-598, 2022.

[2] J. Xu *et al.*, "Forming novel texture and enhancing the formability in Mg–3Al–Zn alloy sheets fabricated by transverse gradient extrusion," *Journal of Materials Research and Technology*, vol. 18, pp. 3143-3149, 2022.

[3] Z.-J. Li *et al.*, "Effect of Ce addition on hot deformation behavior and microstructure evolution of AZ80 magnesium alloy," *Journal of Materials Research and Technology,* vol. 16, pp. 1339-1352, 2022.

[4] J. Koike *et al.*, "The activity of non-basal slip systems and dynamic recovery at room temperature in fine-grained AZ31B magnesium alloys," *Acta materialia,* vol. 51, no. 7, pp. 2055-2065, 2003.

[5] R. Sabat, A. Brahme, R. Mishra, K. Inal, and S. Suwas, "Ductility enhancement in Mg-0.2% Ce alloys," *Acta Materialia,* vol. 161, pp. 246-257, 2018.

[6] Z. Yu, C. Xu, J. Meng, X. Zhang, and S. Kamado, "Microstructure evolution and mechanical properties of as-extruded Mg-Gd-Y-Zr alloy with Zn and Nd additions," *Materials Science and Engineering: A,* vol. 713, pp. 234-243, 2018.

[7] M. Yuan *et al.*, "Microstructure evolution and mechanical properties of the Mg-Sm-Gd-Zn-Zr alloy during extrusion," *Journal of Materials Research and Technology,* vol. 15, pp. 2518-2528, 2021.

[8] L. Yang *et al.*, "Mechanical and corrosion properties of binary Mg–Dy alloys for medical applications," *Materials Science and Engineering: B,* vol. 176, no. 20, pp. 1827-1834, 2011.

[9] G. Zhang *et al.*, "Homogenization heat treatment of Mg-7.68 Gd-4.88 Y-1.32 Nd-0.63 Al-0.05 Zr alloy," *Journal of Rare Earths,* vol. 32, no. 5, pp. 445-450, 2014.

[10] Q. Peng, L. Wang, Y. Wu, and L. Wang, "Structure stability and strengthening mechanism of die-cast Mg–Gd–Dy based alloy," *Journal of Alloys and Compounds,* vol. 469, no. 1-2, pp. 587-592, 2009.

[11] M. Khan, F. Mirza, and R. Gupta, "High hardness and thermal stability of nanocrystalline Mg–Al alloys synthesized by the high-energy ball milling," *Materialia,* vol. 4, pp. 406-416, 2018.

[12] T. P. Yadav, R. M. Yadav, and D. P. Singh, "Mechanical milling: a top down approach for the synthesis of nanomaterials and nanocomposites," *Nanoscience and Nanotechnology,* vol. 2, no. 3, pp. 22-48, 2012.

[13] Z. H. Loh, A. K. Samanta, and P. W. S. Heng, "Overview of milling techniques for improving the solubility of poorly water-soluble drugs," *Asian journal of pharmaceutical sciences,* vol. 10, no. 4, pp. 255-274, 2015.

[14] C. Suryanarayana, "Mechanical alloying: a critical review," *Materials Research Letters,* vol. 10, no. 10, pp. 619-647, 2022.

[15] C. Suryanarayana, "Mechanical alloying and milling," *Progress in materials science,* vol. 46, no. 1-2, pp. 1-184, 2001.

[16] S. J. Huang, A. Muneeb, A. Abbas, and R. Sankar, "The effect of Mg content and milling time on the solid solubility and microstructure of Ti–Mg alloys processed by mechanical milling," *Journal of Materials Research and Technology,* vol. 11, pp. 1424-1433, 2021.

[17] A. Kanatzia, C. Papageorgiou, C. Lioutas, and T. Kyratsi, "Design of ball-milling experiments on Bi2Te3 thermoelectric material," *Journal of electronic materials,* vol. 42, no. 7, pp. 1652-1660, 2013.

[18] M. Phasha, K. Maweja, and C. Babst, "Mechanical alloying by ball milling of Ti and Mg elemental powders: Operation condition considerations," *Journal of alloys and compounds,* vol. 492, no. 1-2, pp. 201-207, 2010.

[19] L. Shaw, J. Villegas, H. Luo, M. Zawrah, and D. Miracle, "Effects of process-control agents on mechanical alloying of nanostructured aluminum alloys," *Metallurgical and Materials Transactions A,* vol. 34, no. 1, pp. 159-170, 2003.

[20] L. Lu and Y. Zhang, "Influence of process control agent on interdiffusion between Al and Mg during mechanical alloying," *Journal of alloys and compounds,* vol. 290, no. 1-2, pp. 279-283, 1999.

[21] M. S. Lamoglia, P. H. Gonçalves, Á. M. P. Pontes, L. B. Serrano, G. Silva, and A. A. A. P. d. Silva, "Effect of Process control agents on Fe-15at.% Nb powder during mechanical alloying," *Materials Research,* vol. 25, p. e20210318, 2022.

[22] H. A. Baghbaderani, S. Sharafi, and M. D. Chermahini, "Investigation of nanostructure formation mechanism and magnetic properties in Fe45Co45Ni10 system synthesized by mechanical alloying," *Powder Technology,* vol. 230, pp. 241-246, 2012.

[23] E. Salur, M. Acarer, and İ. Şavkliyildiz, "Improving mechanical properties of nano-sized TiC particle reinforced AA7075 Al alloy composites produced by ball milling and hot pressing," *Materials Today Communications,* vol. 27, p. 102202, 2021.

[24] A. Restrepo *et al.*, "Characterization of titanium powders processed in n-hexane by high-energy ball milling," *The International Journal of Advanced Manufacturing Technology,* vol. 110, no. 7, pp. 1681-1690, 2020.

[25] S. Kamrani, D. Penther, A. Ghasemi, R. Riedel, and C. Fleck, "Microstructural characterization of Mg-SiC nanocomposite synthesized by high energy ball milling," *Advanced Powder Technology,* vol. 29, no. 7, pp. 1742-1748, 2018.

[26] B. Neamţu, H. Chicinaş, T. Marinca, O. Isnard, O. Pană, and I. Chicinaş, "Amorphisation of Fe-based alloy via wet mechanical alloying assisted by PCA decomposition," *Materials Chemistry and Physics,* vol. 183, pp. 83-92, 2016.

[27] Y. Duan, H. Pang, X. Wen, X. Zhang, and T. Wang, "Microwave absorption performance of FeCoNiAlCr0. 9 alloy powders by adjusting the amount of process control agent," *Journal of Materials Science & Technology,* vol. 77, pp. 209-216, 2021.

[28] J. K. Rana, D. Sivaprahasam, K. S. Raju, and V. S. Sarma, "Microstructure and mechanical properties of nanocrystalline high strength Al–Mg–Si (AA6061) alloy by high energy ball milling and spark plasma sintering," *Materials Science and Engineering: A,* vol. 527, no. 1-2, pp. 292-296, 2009.

[29] M. Ullah, M. E. Ali, and S. B. Abd Hamid, "Surfactant-assisted ball milling: a novel route to novel materials with controlled nanostructure-a review," *Reviews on Advanced Materials Science,* vol. 37, 2014.

[30] L. Zhang and X. Guo, "Effects of process control agents on the mechanical alloying behavior of Nb-Ti-Si based alloy," *Materials Transactions,* vol. 59, no. 4, pp. 528-537, 2018.

[31] M. Trautmann, H. Ahmad, and G. Wagner, "Influencing the size and shape of high-energy ball milled particle reinforced aluminum alloy powder," *Materials,* vol. 15, no. 9, p. 3022, 2022.

[32] C. Machio, H. Chikwanda, and S. Chikosha, "Effect of process control agent (PCA) on the characteristics of mechanically alloyed Ti-Mg powders," *Journal of the Southern African Institute of Mining and Metallurgy,* vol. 111, no. 3, pp. 149-153, 2011.

[33] C. Suryanarayana and E. Ivanov, "Mechanochemical synthesis of nanocrystalline metal powders," in *Advances in powder metallurgy*: Elsevier, 2013, pp. 42-68.

[34] V. Mihalache, G. Aldica, I. Pasuk, and I. Mercioniu, "Thermal analysis and microstructure of oxide dispersion strengthened ferritic steels produced by ball milling with different amounts of process control agent," *Journal of Thermal Analysis and Calorimetry,* vol. 138, pp. 2515-2528, 2019.

[35] B. P. Rocky, C. R. Weinberger, S. R. Daniewicz, and G. B. Thompson, "Carbide nanoparticle dispersion techniques for metal powder metallurgy," *Metals,* vol. 11, no. 6, p. 871, 2021.

[36] S. Motozuka, H. Sato, H. Kuwata, M. Bito, and Y. Okazaki, "Effects of interfacial interactions between metal and process control agents during ball milling on the microstructure of the milled Fe-based nanocrystalline alloy powder," *Heliyon,* vol. 8, no. 8, 2022.

[37] L. K. Wei *et al.*, "Producing metal powder from machining chips using ball milling process: A review," *Materials,* vol. 16, no. 13, p. 4635, 2023.

[38] P. Joshi, G. Marathe, A. Pratap, and V. Kurup, "Effect of addition of process control agent (PCA) on the nanocrystalline behavior of elemental silver during high energy milling," in *IWNMS 2004: Proceedings of the International Workshop on Nanomaterials, Magnetic Ions and Magnetic Semiconductors Studied Mostly by Hyperfine Interactions (IWNMS 2004) held in Baroda, India, 10–14 February 2004*, 2005: Springer, pp. 173-180.

[39] J.-H. Ryu and D. N. Lee, "The effect of precipitation on the evolution of recrystallization texture in AA8011 aluminum alloy sheet," *Materials Science and Engineering: A,* vol. 336, no. 1-2, pp. 225-232, 2002.

[40] H. Sübütay, "Mekanik alaşımlama ile üretilen Mg (1-X) SnX alaşımlarının mekanik ve invivo özelliklerinin incelenmesi," Doktora Tezi, Metalurji ve Malzeme Mühendisliği Selçuk Üniversitesi, Konya, 2023.